Research article

Antioxidative and anti-cytogenotoxic potential of *Lysiphyllum strychnifolium* (Craib) A. Schmitz extracts against cadmium-induced toxicity in human embryonic kidney (HEK293) and dermal fibroblast (HDF) cells

Pattaravan Maliyam [a], Surat Laphookhieo [b], Preeyaporn Koedrith [c], Panupong Puttarak [a,d,*]

[a] *Department of Pharmacognosy and Pharmaceutical Botany, Faculty of Pharmaceutical Sciences, Prince of Songkla University, Hat-Yai District, Songkhla, 90112, Thailand*
[b] *Center of Chemical Innovation for Sustainability (CIS) and School of Science, Mae Fah Luang University, Chiang Rai, 57100, Thailand*
[c] *Faculty of Environment and Resource Studies, Mahidol University, Phuttamonthon District, NakhonPathom, 73170, Thailand*
[d] *Phytomedicine and Pharmaceutical Biotechnology Excellence Center, Faculty of Pharmaceutical Sciences, Prince of Songkla University, Hat-Yai District, Songkhla, 90112, Thailand*

ARTICLE INFO

ABSTRACT

Exposure to cadmium (Cd) results in bioaccumulation and irreversible damage; this encourages an investigation of alternatives to address Cd toxicity, using natural compounds. *Lysiphyllum strychnifolium*, a well-known Thai medicinal plant, was investigated for its phytochemical compounds and corresponding bioactivities, including antioxidant and anti-cytogenotoxic effects against Cd toxicity in HEK293 renal and HDF dermal cell models. The crude extract of *L. strychnifolium* (LsCrude) was partitioned into four fractions, using sequential polarity solvents (hexane, dichloromethane, ethyl acetate, and water, denoted as LsH, LsD, LsE, and LsW, respectively). The extraction yields were 1.79 %, 5.08 %, 8.53 %, and 70.25 % (w/w), respectively. Phytochemical screening revealed the presence of tannins, alkaloids, and flavonoids in LsCrude and its fractions, except for LsH. LsE exhibited the highest concentrations of phenolics (286.83 ± 6.83 mg GAE/g extract) and flavonoids (86.36 ± 1.29 mg QE/g extract). Subsequent 2,2-diphenyl-1-picrylhydrazyl (DPPH) radical-scavenging and ferric-reducing ability of plasma (FRAP) reducing powder assays demonstrated the high antioxidant capacity of LsCrude and its fractions. The lowest IC_{50} value (9.11 ± 0.43 μg/mL) in the DPPH assay corresponded to LsW, whereas the highest total FRAP value (6.06 ± 0.70 mg QE Eq./g dry mass) corresponded to LsE. MTT and alkaline comet assays revealed the lack of toxicity of the extracts, which were considered safe. Upon exposure to Cd at the CC_{50} level, HEK293 cells treated with LsE suppressed Cd-induced damage. HDF cells treated with LsCrude, LsD, or LsE attenuated Cd-induced damage. In the pre-treatment, LsD protected the HDF cells against Cd-mediated cytogenotoxicity. These anti-cytogenotoxic potentials are likely due to the antioxidant properties of the phytochemicals. Our findings highlight the cyto-geno-protective properties of *L. strychnifolium* stem extracts against Cd toxicity in HEK293 and HDF cells, and provide a novel approach for combating oxidative stress and DNA damage caused by environmental pollutants.

---

* Corresponding author.
E-mail address: panupong.p@psu.ac.th (P. Puttarak).

Abbreviation list

AA	Ascorbic acid
ANOVA	Analysis of variances
ATP	Adenosine triphosphate
CAT	Catalase
CC_{50}	50 % Cytotoxic concentration value
Cd	Cadmium
CO_2	Carbon dioxide
DMEM	Dulbecco's Modified Eagle Medium
DMSO	Dimethyl sulfoxide
DNA	Deoxyribonucleic acid
DPPH	2, 2-diphenyl-1-picrylhydrazyl
EtOH	Ethanol
FBS	Fetal Bovine serum
Fe^{2+}	Ferrous cation
Fe^{3+}	Ferric cation
$FeCl_3$	Ferric chloride
FRAP	Ferric reducing antioxidant power
GPx	Glutathione peroxidase
H_2SO_4	Sulfuric acid
HDF cells	Human dermal fibroblasts cells
HEK293 cells	Human epithelial kidney cells
HeLa cells	Human cervical adenocarcinoma cells
HT-29 cells	Human colorectal adenocarcinoma cells
IC_{50}	Half maximal inhibitory concentration
$K_3[Fe (CN)_6]$	Potassium ferricyanide
KB cells	Human oral epithelial carcinoma cells
KKU-M156 cells	Cholangiocarcinoma cells
LMA	Low melting point agarose
LS174T cells	Human colorectal adenocarcinoma cells
LsD	The fractionation of dichloromethane
LsE	The fractionation of ethyl acetate
LsH	The fractionation of hexane
LsW	The fractionation of water
MCF-7 cells	Human breast cancer cells
MDA	Malondialdehyde
MeOH	Methanol
MTT	3-(4,5-dimethylthiazol-2yl)-2,5-diphenyl tetrazolium bromide
NaOH	Sodium hydroxide
NH_3	Ammonia
NMR	Nuclear magnetic resonance
PAHs	Polycyclic aromatic hydrocarbons
PBS	Phosphate-buffered saline
QE	Quercetin
ROS	Reactive oxygen species
S.D.	Standard deviation
SOD	Superoxide dismutase
SW480	cells Human colon cancer cells

1. Introduction

Modern industries release pollutants into the environment [1]. The extensive use of cadmium (Cd) in industry and commercial activities increases the likelihood of human exposure [2]. Cd, recognized as a highly toxic metal to humans [3,4], can be absorbed through various sources including contaminated soil, drinking water, the food chain, polluted air, cigarette smoke, and children's plastic toys [5]. Previous research indicates that, even at low levels, Cd exposure has detrimental effects on cellular and molecular structures because of its extended half-life (10–30 years) [6,7]. Cd accumulation causes mitochondrial dysfunction, generating reactive oxygen species (ROS). These ROS induce oxidative stress, damaging DNA, proteins, and lipids, triggering cell apoptosis and a decline in organ function [8,9]. The deleterious impact of Cd on DNA includes inducing single- and double-strand breaks in DNA, DNA-protein

crosslinking, chromosomal aberrations, and changes in the expression of proto-oncogenes, thereby increasing the risk of cancer [10]. Cd toxicity is also due to the inhibition of glutathione and key antioxidant enzymes such as superoxide dismutase and glutathione peroxidase. Furthermore, even at low concentrations, Cd suppresses crucial enzymes for DNA repair [11]. A growing body of evidence indicates an interplay among mitochondrial dysfunction, an imbalance in oxidant-antioxidant levels, and the DNA damage response and repair system. Oxidative stress emerges as a unifying mechanism associated with Cd-mediated damage to cells and DNA.

The kidney is a vulnerable organ affected by Cd toxicity [12]. Approximately half of the total Cd load in the body accumulates in the epithelial cells of the kidney's proximal tubule, leading to proteinuria and a disrupted reabsorption process [13]. Chronic exposure to Cd also augments calcium excretion and the risk of kidney stones [14]. Numerous studies have documented the onset of acute and chronic kidney diseases, even at low levels of Cd exposure. Populations with confounding health conditions like diabetes and obesity are particularly susceptible [15,16]. There is a clear association between Cd exposure and renal dysfunction, leading to kidney damage [17]. Thus, strategies to mitigate Cd-induced kidney injury should be developed.

The skin, the body's largest organ, is also a target for Cd toxicity. The skin acts as a complex protective barrier against external threats and moisture loss through physical and chemical defenses [18]. Cd pollution can interfere with this barrier function, resulting in apoptosis, DNA damage, and lipid oxidation [19]. Concurrently, antioxidant enzymes in the skin, including glutathione peroxidase and methionine sulfoxide reductase, are disrupted [20]. The primary mechanism underlying the detrimental effects of Cd is the induction of oxidative stress, leading to skin senescence and disrupting skin homeostasis [21,22].

Lysiphyllum strychnifolium (W. G. Craib) A. Schmitz (a member of the Fabaceae family), also known as *Bauhinia strychnifolia* Craib., is a common medicinal plant in Thailand, where it is called Ya nang daeng. This herb is used in traditional medicine to treat fever and alcoholic intoxication and as an antidote against pesticide poisoning. The antioxidant properties of the leaf and stem extracts align with the plant's traditional uses, supporting its role in detoxification and alleviating chronic ailments [23,24]. The infusion of *L. strychnifolium* has shown notable biological activities, including an increase in cholinesterase levels in farmers exposed to pesticides [24]. The infusion of *L. strychnifolium* is rich in phenols and has also exhibited antioxidant properties [23,25,26]. Some chemical constituents derived from the ethanolic extract of the *L. strychnifolium* stem exhibited inhibitory effects against various cancer cells [27, 28]. Notably, 3,5,7,3′,5′-pentahydroxyflavanonol-3-*O*-α-ʟ-rhamnopyranoside demonstrated efficacy against mouth (KB), colon (HT-29), breast (MCF-7), and cervical (HeLa) adenocarcinoma cells [27]. Furthermore, 3,5,7-trihydroxychromone-3-*O*-α-ʟ-rhamnopyranoside inhibited KB, HT-29, and MCF-7 cancer cells [27]. Other bioactive molecules (antioxidants) identified in both leaves and stems of *L. strychnifolium* include gallic acid, trilobatin, yanangdaengin, and astilbin [29]. Moreover, 25 flavonoids and eight phenolics were identified in the ethyl acetate fraction of this plant, using liquid chromatography-quadrupole time-of-flight mass spectrometry (LC-QTOF/MS) [30]. These phytochemical components have shown anti-genotoxic potential against Cd, with flavonoids such as catechin, quercetin, and resveratrol exhibiting noteworthy effects [31–33]. Despite numerous studies recommending the use of *L. strychnifolium* or its extracts for their detoxification properties, a knowledge gap remains concerning their safety and potential DNA-protective effects against environmental toxicants such as Cd or other toxic metals.

Hence, this study aimed to determine the antioxidant and protective effects against Cd of a 95 % ethanolic extract from *L. strychnifolium* stems and its fractions (hexane, dichloromethane, ethyl acetate, and water). The cytoprotective and antigenotoxic potentials of these extracts against Cd-induced damage were evaluated at their half-maximal inhibitory concentrations (IC$_{50}$), using the MTT assay and alkaline comet assay, respectively. This study represents the first investigation of the anti-cytogenotoxic effects of *L. strychnifolium,* using human embryonic kidney (HEK293) and human dermal fibroblast (HDF) cells as representative models for renal and dermal systems, respectively. In addition, the *L. strychnifolium* extracts that exhibited high anticytotoxic and antigenotoxic activities were identified. Our findings reveal the potential use of *L. strychnifolium* as an alternative treatment for reducing Cd toxicity. The active compounds isolated from this plant should be evaluated in further studies.

2. Materials and methods

2.1. Reagents

Analytical-grade ethanol, methanol, hexane, dichloromethane, and ethyl acetate were purchased from Labscan Asia Co., Thailand. Ascorbic acid and quercetin acquired from Sigma Aldrich, Switzerland were used as standards for the 2, 2-diphenyl-1-picrylhydrazyl (DPPH) radical scavenging assay and the ferric reducing antioxidant power (FRAP) assay, respectively. The reagents and media used for the cell culture included Dulbecco's Modified Eagle Medium (DMEM), trypsin-EDTA, fetal bovine serum (FBS), penicillin-streptomycin, trypan blue dye, and 3-(4, 5-dimethylthiazol-2-yl)-2, 5-diphenyltetrazolium bromide (MTT) were obtained from Thermo Fisher Scientific Co. (San Jose, CA, USA). Dimethyl sulfoxide (DMSO), low melting point agarose (LMA), and Triton-X were purchased from Amresco Inc. (Solon, OH, USA). SYBR gold nucleic acid stain was acquired from Thermo Fisher Scientific Co. (San Jose, CA, USA).

2.2. Plant materials

L. strychnifolium stems were collected from the herbal garden at Prince of Songkhla University, Thailand, in 2022. The identification of *L. strychnifolium* was confirmed by comparing its appearance to that of the voucher specimen (SKP 2060200-101) kept at the herbarium of the Department of Biology, Faculty of Sciences, Prince of Songkhla University.

2.3. Preparation of crude extracts and compound isolation

L. strychnifolium stems (10 kg) were cleaned, crushed into small pieces, and then dried in a hot air oven at 60 °C for approximately 48 h. The dry sample was subsequently ground into a powder and extracted using 95 % ethanol, maintaining a solid-to-solvent ratio of 1:10 (w/v) (100 L) over 7 days. The powdered stem was mixed with methanol and filtered using Macherey-Nagel Filter Paper MN 751. The filtrate was then evaporated with a rotary evaporator at 45 °C. The maceration process was repeated three times. The resulting crude extract was then partitioned to obtain fractions in the sequence of hexane (LsH), dichloromethane (LsD), ethyl acetate (LsE), and water (LsW), which were keep in well close container and stored at 4 °C for subsequent experiments [27,34,35].

2.4. Phytochemical analysis

Phytochemical analyses of the extracts were performed to identify the presence of tannins, saponins, alkaloids, flavonoids, triterpenoids, coumarins, anthraquinones, and steroids using standard methods [36–39].

2.4.1. Tannins
The LsCrude and its fractions (10 mg/mL each) were separately stirred with distilled water (20 mL) in a water bath and then filtered. A few drops of 1 % w/v ferric chloride were then added. The presence of a black or blue-green color or precipitate was interpreted as a positive result for tannins.

2.4.2. Saponins
The LsCrude and its fractions (10 mg/mL each) were separately shaken with distilled water (5 mL) in a test tube. After heating in a water bath for 5 min, the formation and persistence of foam, indicate the presence of saponins.

2.4.3. Alkaloids
A solution of 10 % H_2SO_4 (2 mL) was added to the LsCrude and its fractions (10 mg/mL each), and the blends were heated in a water bath for 5 min, followed by filtration. Subsequently, a small amount of Dragendorff's reagent, a solution containing potassium bismuth iodide, was added. The appearance of an orange-red precipitate signified the presence of alkaloids.

2.4.4. Flavonoids
The LsCrude and its fractions (10 mg/mL each) were separately stirred with 50 % ethanol (0.5 mL) and then filtered. A small piece of magnesium was added, followed by 3–5 drops of concentrated hydrochloric acid, with the formation of a reddish or brown color indicating the presence of flavonoids.

2.4.5. Triterpenoids
The LsCrude and its fractions (10 mg/mL each) were boiled with EtOH (20 mL) in a test tube and then filtered. The filtrate was then placed in an evaporating dish and allowed to permit it to undergo dry in a water bath. Thereafter, a few drops of concentrated H_2SO_4 were introduced, with the appearance of a reddish hue denoting the presence of steroid triterpenoids.

2.4.6. Coumarins
The LsCrude and its fractions (10 mg/mL each) were transferred into a 5-mL test tube, which was sealed with 10 % NaOH-coated filter paper and heated in a water bath at 60 °C for 10 min. The filter paper was examined under UV light at 365 nm; the presence of volatile coumarins was suggested by the existence of greenish-blue spots.

2.4.7. Anthraquinones
After combining the LsCrude and its fractions (10 mg/mL each) with 10 % H_2SO_4 (2 mL), the mixtures were boiled in a water bath for 5 min and then filtered. The filtrate was then shaken with 1 mL of diethyl ether; the layer of diethyl ether was then separated and shaken with 1 mL of 10 % NH_3, with the formation of a rose pink to red color in the ammoniacal layer indicating the presence of anthraquinone glycosides.

2.4.8. Steroids
The LsCrude and its fractions (10 mg/mL each) were separately boiled with EtOH (20 mL) and then filtered. Glacial acetic acid (0.5 mL) was then added, followed by the addition of a few drops of concentrated H_2SO_4 along the sides of the test tube; a blue or green color at the interface signified the presence of a steroid.

2.5. Total phenolic contents (TPC)

To assess the total phenolic content in both LsCrude and its fractions (LsH, LsD, LsE, and LsW) a method was employed [40]. Initially, 25 µl of the extract (1 mg/mL), diluted in DMSO, was combined with 125 µL of 10 % Folin-Ciocalteu reagent (v/v) and allowed to incubate for 2 min. Subsequently, 100 µl of a 7.5 % (w/v) Na_2CO_3 solution was introduced into the mixture, followed by a 30-min incubation period at room temperature. The absorbance was then measured using a UV–Vis spectrophotometer at a wavelength of 765 nm. To establish a calibration curve, gallic acid at various concentrations (0–500 µg/mL) as a referent standard. The results are

reported as mg of gallic acid equivalent/mg extract (mg GAE/mg extract).

2.6. Total flavonoid contents (TFC)

The total flavonoid content was assessed using the aluminum chloride method [41]. Samples of LsCrude and its fractions (LsH, LsD, LsE, and LsW) were prepared by extracting them in DMSO to a concentration of 1 mg/mL. Each sample (300 μL) was then transferred to a 1.5 mL test tube, to which 20 μL of aluminum chloride solution (10 % $AlCl_2$) was added. After 5 min of incubation at room temperature, 20 μL of 1 M potassium acetate (CH_3COOK) was added to the mixture. After another 5 min, each reaction was diluted with 560 μL of distilled water and incubated for 30 min. The absorbance of the reaction mixtures was measured at 510 nm. Quercetin in DMSO was used as a standard with concentrations ranging from 0 to 500 μg/mL. The total flavonoid content was expressed as mg quercetin equivalent (QE) per gram of sample dry matter (mg QE/g DW).

2.7. Determination of the free radical scavenging potential of the extracts

2.7.1. DPPH radical scavenging activity assay

This study aimed to evaluate the capacity of the LsCrude and its fractions to attenuate free radicals. A consistent example of a free radical molecule is DPPH. When an antioxidant is present, it can donate electrons to DPPH, causing the usual purple color of the molecule to fade; this transformation in absorbance is quantified at a wavelength of 517 nm. The antioxidant activity of the plant extracts was assessed by utilizing the DPPH stable free radical scavenging effect [42,43]. First, 1 mL of a methanol solution containing 0.1 mM DPPH was added to 3 mL of each diluted extract (1 mg/mL) or ascorbic acid (1–100 μg/mL), with the latter used as a standard. The mixtures were incubated in the dark at room temperature for 30 min, and the absorbance at 517 nm was subsequently assessed in comparison to a control sample. The proportion of each extract's radical scavenging capacity was calculated using Equation (1):

$$\text{Scavenging effect } (\%) = 100\% \times (\text{Ao} - \text{As})/\text{Ao}, \tag{1}$$

where Ao is the absorbance of the blank, and As is the absorbance of the sample. The IC_{50} values were calculated using linear regression analysis and used to indicate the antioxidant capacity.

2.7.2. Ferric reducing antioxidant power (FRAP) assay

The reducing capabilities of LsCrude and its fractions were also assessed [42]. First, 200 μL aliquots of the extract (200 μg/mL) or quercetin (0.5–100 μg/mL; used as a standard), prepared in MeOH, were mixed with 500 μL portions of a 2 M phosphate buffer (pH 6.6) and 500 μL portions of 1 % potassium ferricyanide, $K_3[Fe (CN)_6]$. The mixtures were incubated for 20 min at 50 °C; thereafter, 500 μL of a 10 % trichloroacetic acid solution was introduced, and the resultant mixtures were then centrifuged at 3000 rpm for 10 min. The upper layer (600 μL) of the solution was mixed with 120 μL of a 0.1 % ferric chloride ($FeCl_3$) solution and 600 μL of distilled water, after which the absorbance at 700 nm was recorded. The reducing power of each sample was quantified in terms of the quercetin equivalent. All experiments were conducted in triplicate.

2.8. Cell culture model

HEK293 and HDF cells were purchased from the American Type Culture Collection (Manassas, VA, USA). The cell culture medium consisted of DMEM supplemented with 10 % FBS, 1.5 % sodium bicarbonate, and 1 % penicillin-streptomycin. The cultures were incubated in a 5 % CO_2 atmosphere at 37 °C. Throughout the entire experiment, phosphate-buffered saline (PBS) with a pH of 7.2 was used for washing the cells to maintain their condition.

2.8.1. Cell viability using MTT assay

Cell viability was assessed using MTT assay. The HEK293 and HDF cells were seeded in 96-well plates at a density of 1×10^4 [44] and 5×10^3 cells/well [45], respectively. After 24 h, doses of the LsCrude and its fractions (20–100 μg/mL) were added to each cell line up to a final volume of 200 μL. Cell viability was assessed 24 h later by introducing 20 μL of MTT solution, prepared from a 5 mg/mL stock solution, and incubating the cells at 37 °C for 2 h. The formazan crystals were solubilized with 100 μL DMSO, and the formazan content was then determined by measuring the absorbance at a wavelength of 570 nm using a microplate reader. Equation (2) was employed to determine the percentage cell viability:

$$\% \text{ Cell viability} = (\text{Absorbance of sample} / \text{Absorbance of control}) \times 100\%, \tag{2}$$

2.8.2. Evaluation of cytotoxicity and anti-cytotoxicity using MTT assay

The cytotoxic doses of a damaging agent, cadmium chloride ($CdCl_2$), and anti-cytotoxicity of the LsCrude and its fractions against Cd-induced damage were evaluated in HEK293 and HDF cells. Half-maximal cytotoxicity concentration (CC_{50}) of $CdCl_2$ as suggested dose for inducing cytotoxicity was initially determined. The HEK293 and HDF cells were seeded at a density of 1×10^4 [44] and 5×10^3 cells/well in 96-well plates [45], respectively. After 24 h, each cell line was treated with $CdCl_2$ or the LsCrude and its fractions. Herein, the treatment conditions were classified into three modalities, distinguished by specific time sequences for administering the extracts to the cells [46] as follows: 1) **pre-treatment:** cells were prior exposed to varying concentrations of the LsCrude and its fractions for 24 h, followed by a new culture medium containing $CdCl_2$ at the CC_{50} (μM) level for an additional 24 h this period after the

removal of the old medium; 2) **co-treatment:** cells were simultaneously exposed to the LsCrude and its fractions, along with CdCl$_2$ at the CC$_{50}$ (μM) level for 24 h; 3) **post-treatment:** cells were initially exposed to CdCl$_2$ at the CC$_{50}$ (μM) level for 24 h, followed by a new culture medium containing indicated concentrations of the LsCrude and its fractions for an additional 24 h after the removal of the old medium. The MTT assay was employed to assess the cell viability [44], by which is calculated according to Equation (2) (as mentioned in subtopic 2.6.1).

2.8.3. Assessment of genotoxicity and anti-genotoxicity using in vitro alkaline comet assay

The comet assay, an alkaline single-cell gel electrophoresis technique, was employed to assess DNA damage by investigating the DNA protective properties of the LsCrude and fractions with respect to the CdCl$_2$-exposed HEK293 and HDF cells. First, the HEK293 and HDF cells were seeded in 12-well plates at a density of 1×10^4 and 5×10^3 cells/well, respectively, and then incubated at 37 °C for 24 h. They were subsequently subjected to the described treatment and then harvested and fixed onto slides, which featured an initial layer of a 1.5 % LMA solution (150 μL). After this layer had solidified, second layer (80 μL), composed of a mixture created by rapidly pipetting 20 μL of a freshly prepared cell suspension into 180 μL of a 0.5 % LMA solution (in a 1:9 ratio), was applied. Thereafter, a third layer, comprising of 70 μL of a 1.0 % LMA solution, was added on top of the cell layer. After the gel had set, the slides were incubated for at least 2 h at 4 °C in a cooled lysis solution (pH 10). Following the removal of the slides, the DNA was unwound via immersion in an electrophoresis tank (Model CSL-COM20, Cleaver Scientific, UK) containing a freshly prepared alkaline buffer (pH $\geq$ 13) at 4 °C for 15 min. Electrophoresis was then performed at 25 V and 300 mA for 45 min. The slides were subsequently delicately balanced via exposure to a 0.4 M Tris-HCl buffer at a pH of 7.5 for 5 min, which was followed by a thorough rinse with deionized water. After a 5-min soak in ethanol and storage at room temperature, the slides were allowed to air dry completely. The cellular DNA was then stained with SYBR gold nucleic acid stain in a dark environment for 20 min using a fluorescence microscope (Nikon Eclipse TS100, excitation wavelength range between 450 and 490 nm). A total of 100 cells per slide were imaged and subsequently analyzed. The comet-like DNA damage was scored by five-point scaling as follows: Type 0 (undamaged), Type I (low-level damage), Type II (medium-level damage), Type III (high-level damage), and Type IV (complete damage). The percentage of tail DNA categorized as Types II, III, or IV was employed to quantify the degree of DNA damage [44,47,48].

2.9. Liquid chromatography with tandem mass spectrometry (LC-MS/MS) analysis

The extracts demonstrating significant efficacy against DNA damage were analyzed using a modified method by Praparatana, R [30]. LC–MS/MS was performed with an Agilent LC-QTOF 6500 system, employing an Agilent ZORBAX Eclipse XDB-C18 column (2.1 × 50 mm, 1.7 μm). The column temperature was maintained at 30 °C. Injection volume was set to 1 μL, and the flow rate was 0.2 mL/min. The mobile phases consisted of water with 0.1 % formic acid (mobile phase A) and acetonitrile with 0.1 % formic acid (mobile phase B), utilized in a gradient mode. The gradient program was as follows: 5 % B for 10 min, 17 % B for 10 min, 95 % B for 5 min, and finally 5 % B for 8 min.

The UPLC system was interfaced with a QTOF mass spectrometer (6500 series, Model G6545B, Agilent Technologies, Santa Clara, CA, USA) equipped with a Dual AJS ESI source. The MS was operated with the Dual AJS ESI, and the parameters were: gas temperature at 300 °C, gas flow at 10 L/min, nebulizer pressure at 35 psi, sheath gas temperature at 350 °C, sheath gas flow at 11 L/min, VCap at 3500 V, nozzle voltage at 1000 V, fragmentor voltage at 175 V, skimmer1 at 65 V, and octopole RF peak at 750. The ion trap scan range was 100–1100 *m/z* for MS and 50–1100 *m/z* for MS/MS. Mass spectra were recorded in both negative and positive ion modes. Initial LC/MS data processing was performed using Agilent MassHunter Qualitative Analysis Software version 10.00. Compound identification was facilitated by the Molecular Feature Extractor (MFE) tool within the software. The Agilent Metlin Metabolite Personal Compound Database and Library (PCDL) version 5.0 was employed for compound identification based on MS/MS spectra matching.

2.10. Statistical analysis

In the statistical analysis, the data were presented as the mean (n = 3) ± standard deviation (S.D.). Group comparisons were conducted using a one-way analysis of variance (ANOVA) with SPSS software (SPSS Inc., Chicago, IL, USA). To identify significant differences ($p < 0.05$), Tukey's range test was applied.

3. Results and discussion

3.1. Extraction of L. strychnifolium (Ls) stems

The dried powder of *L. strychnifolium* stems was macerated with 95 % ethanol, resulting in an extraction yield of 17.95 % (w/w). The crude ethanolic extract has been traditionally used in the treatment of ailments, such as cancer and pesticide poisoning [23, 24]. The crude extract (LsCrude) was assessed for its phytochemical composition and bioactivities, including cytoprotective and anti-genotoxic effects. Subsequently, LsCrude was partitioned using four solvents based on polarity (hexane, dichloromethane, ethyl acetate, and water), producing four fractions: LsH, LsD, LsE, and LsW, with extraction yields of 1.79 %, 5.08 %, 8.53 %, and 70.25 % (w/w), respectively. The phytochemicals were more soluble in high-polarity solvents than in moderate- or low-polarity ones, consistent with our earlier research [30]. In a previous study [27], the fractions extracted using hexane, ethyl acetate, chloroform, and water represented 0.5 %, 15.5 %, 5.9 %, and 46.2 % (w/w), respectively. This indicates that high-polarity solvents result in high extraction

yields**.** These fractions were evaluated for their cytoprotective and antigenotoxic effects against Cd-induced damage and were compared to LsCrude in subsequent experiments.

3.2. Phytochemical screening of the L. strychnifolium crude extract and its fractions

The ethanolic crude extract of *L. strychnifolium* stem and its fractions were subjected to phytochemical screening, revealing the presence of various secondary metabolites, including alkaloids, flavonoids, tannins, saponins, and steroids. Tannins, alkaloids, and flavonoids were identified in both LsCrude and the LsW fraction. These three phytochemicals, along with steroids, were detected in the LsD and LsE fractions. The LsH fraction contained saponins, alkaloids, and steroids (Table 1). These phytochemical compounds are known for their bioactivities, explaining the observed antioxidant effects [49].

In our previous investigation on the anti-diabetic activity of the *L. strychnifolium* crude ethanolic extract and its fractions through bioassay-guided isolation, flavonoids were identified in the ethyl acetate and water fractions. The water fraction contained quercetin and 3,5,7-trihydroxy-chromone-3-*O*-α-L-rhamnopyranoside, whereas the ethyl acetate fraction contained 3,5,7-trihydroxy-chromone-3-*O*-α-L-rhamnopyranoside and 3,5,7,3′,5′-pentahydroxyflavanonol-3-*O*-α-L-rhamnopyranoside. Furthermore, the hexane fraction contained steroid compounds, namely a mixture of β-sitosterol and stigmasterol [27,50]. Thus, these phytochemicals may be present in the LsCrude and its fractions, possibly contributing to the antioxidant activities and consequent cytoprotective and antigenotoxic potential.

3.3. Total phenolic contents (TPC) and total flavonoid contents (TFC)

To screen for bioactive compounds, we assessed the TPC and TFC of the crude extract and four fractions, using colorimetric assays. The TPC value was determined using a gallic acid calibration curve ($y = 0.0058x + 0.0442$, $R^2 = 0.9999$) and expressed as milligrams of gallic acid equivalent per gram of extract (mg GAE/g extract). The TFC value was obtained from a quercetin calibration curve ($y = 0.0009x + 0.0406$, $R^2 = 0.9979$) and expressed as milligrams of quercetin equivalent per gram of extract (mg QE/g extract). The highest concentrations of both TPC and TFC were observed in LsE (286.83 ± 6.83 mg GAE/g extract), followed by LsCrude (242.34 ± 10.21 mg GAE/g extract), LsW (210.85 ± 18.13 mg GAE/g extract), LsD (200.36 ± 2.53 mg GAE/g extract), and only trace amounts were found in LsH (19.53 ± 0.79 mg GAE/g extract) (Table 2). Similarly, the TFC values revealed that LsE had the highest concentration (86.36 ± 1.29 mg QE/g extract), followed by LsCrude (55.63 ± 0.62 mg QE/g extract), LsW (53.48 ± 0.46 mg QE/g extract), and LsD (41.64 ± 0.30 mg QE/g extract).

The qualitative phytochemical screening revealed the presence of flavonoids in the LsCrude, LsD, LsE, and LsW extracts, which aligns with the TPC and TFC values observed. These values are comparable to those previously reported by Praparatana, R. et al. [30]. Likewise, Itharat A. et al. found that the crude extract of *L. strychnifolium* stems had a high total phenolic content [26]. Our results corroborate these findings, suggesting that the high levels of flavonoids and phenolic components in LsCrude, LsD, LsE, and LsW may contribute to their potent antioxidant activity and their inhibitory effects on cytotoxic and genotoxic activities.

3.4. In vitro antioxidant activities of the LsCrude extract and its fractions, determined by the DPPH and FRAP assays

Two methods were applied to assess the antioxidant activities: the DPPH radical-scavenging activity and FRAP reducing-capability assays. The degree of reduction in the absorbance measurement indicates the scavenging capacity of the tested compounds. Therefore, we evaluated the free radical-scavenging activity of LsCrude and its fractions, comparing them to reference standards, namely, ascorbic acid and quercetin in the DPPH and FRAP assays, respectively (Table 2).

The DPPH assay measures a compound's ability to act as a hydrogen atom or electron donor for converting the DPPH radical into its reduced form, DPPH-H [51]. Ascorbic acid (AA) served as the reference standard [52], and the results were expressed as IC_{50} values (µg/mL). Table 2 reveals that LsCrude and its fractions, excluding LsH, reduced the stable purple-colored DPPH radical to its yellow-colored form (DPPH-H) by 50 %. LsW exhibited the lowest IC_{50} value (9.11 ± 0.43 µg/mL), followed by LsE (22.80 ± 0.94 µg/mL), LsD (24.03 ± 1.07 µg/mL), and LsCrude (43.82 ± 1.21 µg/mL), with ascorbic acid serving as the reference standard (2.24 ± 0.17 µg/mL). This result suggests a substantial antioxidant capacity in LsCrude and its fractions, aligning with previous research that reported a high antioxidant capacity ($IC_{50} > 10$–50 µg/mL) [53]. We consider that the antioxidant capacity of *L. strychnifolium* is linked

Table 1

Qualitative phytochemical screening of LsCrude and its partitioned fractions.

Phytochemical Test	LsCrude	LsH	LsD	LsE	LsW
Tannin	+	−	+	+	+
Saponins	−	+	−	−	−
Alkaloid	+	+	+	+	+
Flavonoid	+	−	+	+	+
Triterpenoid	−	−	−	−	−
Coumarins	−	−	−	−	−
Anthraquinones	−	−	−	−	−
Steroidal	−	+	+	+	−

(−) not detected/present; (+) present.

Table 2

Qualitative characterization of flavonoids, phenolics and antioxidant activities of *L. strychnifolium* extract and its fractions using DPPH and FRAP assay.

Sample	TPC [mg GAE/g extract]	TFC [mg QE/g extract]	Antioxidant activities	
			DPPH [IC_{50} (µg/mL)]	FRAP (mg QE Eq./g D.M.)
Ascorbic acid	NT	NT	2.24 ± 0.17	NT
LsCrude	242.34 ± 10.21	55.63 ± 0.62	43.82 ± 1.21	5.40 ± 0.53
LsH	19.53 ± 0.79	NA	NA	0.40 ± 0.16
LsD	200.36 ± 2.53	41.64 ± 0.30	24.03 ± 1.07	3.56 ± 0.05
LsE	286.83 ± 6.83	86.36 ± 1.29	22.80 ± 0.94	6.06 ± 0.70
LsW	210.85 ± 18.13	53.48 ± 0.46	9.11 ± 0.43	3.68 ± 0.30

NA = Not active, NT = not performed.

to its phytochemical components [54,55].

The FRAP assay uses the FRAP value as a crucial indicator of a compound's ability to reduce ferric to ferrous ions [56]. Antioxidant activities are often expressed as the quercetin (QE) equivalent value (mg QE Eq./g dry mass). Table 2 shows that LsE exhibited the highest total FRAP value (6.06 ± 0.70 mg QE Eq./g dry mass), followed by LsCrude (5.40 ± 0.53 mg QE Eq./g dry mass), LsW (3.68 ± 0.30 mg QE Eq./g dry mass), LsD (3.56 ± 0.05 mg QE Eq./g dry mass), and LsH (0.40 ± 0.16 mg QE Eq./g dry mass). The antioxidant compounds in LsCrude and its fractions convert iron from its oxidized form (Fe^{3+}) to its reduced form (Fe^{2+}) by donating an electron. This suggests that reductants (used here as synonymous with antioxidants) in the *L. strychnifolium* extracts reduce the Fe^{3+}/ferricyanide complex to the ferrous form. The Perls' Prussian blue technique detects the Fe^{2+} complex at 700 nm, with higher absorbance indicating higher reducing ability [56,57]. Flavonoids, including catechin, epicatechin, quercetin, and rutin, are among the secondary metabolites of *L. strychnifolium* contributing to its antioxidant activity [58,59].

3.5. Intrinsic cytotoxic effects of the LsCrude extract and its fractions on HEK293 and HDF cells, determined by the MTT assay

The MTT assay was used to verify the effect of LsCrude and its fractions on cell viability. HEK293 and HDF cells were used as mammalian cell models for the renal and dermal systems, respectively. The intrinsic cytotoxicity was assessed following the incubation of healthy cells with various concentrations (20–100 µg/mL) of the LsCrude extract and its fractions for 24 h.

LsCrude and its fractions (LsH, LsD, LsE, and LsW) exhibited undetectable or minimal toxicity on HEK293 cells at all specified concentrations (Fig. 1A). All the fractions, except for LsH, stimulated the growth of HEK293 cells.

Similarly, LsCrude and its fractions LsD, LsE, and LsW, showed minimal toxicity on HDF cells (Fig. 1B). LsCrude increased the cell viability of HDF cells in a dose-dependent manner, compared to the untreated control, suggesting enhanced cell proliferation as in the HEK293 cells. By contrast, the LsH fraction exhibited some growth inhibition of the HDF cells. The other fractions had no substantial effects on cell viability. Consistent with previous research, the safe concentration was over 80 % that of the control, even for a lower viable cell count [60].

3.6. Cytoprotective effects of LsCrude and its fractions against Cd toxicity in HEK293 and HDF cells, determined by the MTT assay

The viability of both the HEK293 and HDF cells markedly decreased upon exposure to higher $CdCl_2$ concentrations (Fig. 2). The
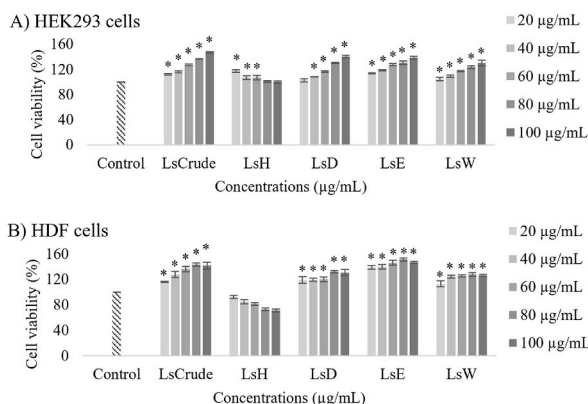

Fig. 1. Intrinsic cytotoxic effects of LsCrude and its partitioned fractions (LsH, LsC, LsE and LsW) at indicated concentrations on A) HEK293 and B) HDF cells. Cytotoxicity, reflecting in cell viability, was determined using MTT assay and expressed as a percentage relative to the untreated control. Each value represents as mean ± standard deviation (n = 3). An asterisk (*) denotes a significant difference between the natural compound-treated group and the control group at a $p < 0.05$.

incubation of HEK293 cells with $CdCl_2$ (0, 20, 40, 60, 80, or 100 μM) for 24 h resulted in a dose-dependent inhibition of cell proliferation, reaching the lowest cell viability (33 %) at 100 μM (Fig. 2A). Exposure to $CdCl_2$ at 40 μM resulted in a relative cell viability of approximately 50 %. Similarly, the incubation of HDF cells with $CdCl_2$ at various concentrations (0, 5, 10, 15, or 20 μM) for 24 h suppressed cell proliferation in a dose-dependent manner, with the lowest cell viability (34 %) observed at 20 μM (Fig. 2B). Exposure to $CdCl_2$ at 10 μM resulted in a relative cell viability of approximately 50 %. Therefore, 40 μM and 10 μM were selected as the half-maximal cytotoxicity concentrations (CC_{50}) for subsequent experiments on HEK293 and HDF cells, respectively.

The MTT assay was used to determine the cytoprotective effects of LsCrude and its fractions against Cd toxicity (CC_{50}) in HEK293 and HDF cells. Three treatment modalities were used: pre-treatment, co-treatment, and post-treatment.

A dose-dependent increase in the viability of HEK293 cells following 24-h co-treatment was observed (Fig. 3). In particular, 100 μg/mL of LsCrude, LsE, or LsW resulted in high cell viability. The cells were co-treated with LsCrude (20–100 μg/mL) along with the CC_{50} (μM) concentration of $CdCl_2$ for 24 h. As a result, cell survival was consistently above 80 % at higher extract concentrations ($\geq$ 60 μg/mL), showing a dose-dependent trend (Fig. 3B). The maximum increase in cell survival corresponded to the 100 μg/mL LsCrude group. Co-treatment with increasing concentrations of LsE or LsW displayed a dose-dependent effect on cell viability (> 80 %) at higher concentrations ($\geq$ 80 μg/mL). By contrast, co-treatment with varying concentrations of LsD resulted in only slightly higher cell viability at higher concentrations (80–100 μg/mL), compared to the Cd-exposed group. On the other hand, co-exposing the HEK293 cells to different LsH concentrations did not affect their viability. As illustrated in Fig. 3A and C, respectively, both pre-exposure and post-exposure of the HEK293 cells to the tested compounds did not attenuate the Cd-mediated decrease in cell viability, compared to those treated solely with $CdCl_2$ at the CC_{50} (μM) level. These findings highlight the distinct effects of LsCrude, LsE, LsW, LsD, and LsH on HEK293 cell viability during the co-treatment with $CdCl_2$. However, neither the pre-treatment nor the post-treatment showed similar effects. This provides valuable insights into the potential cell proliferative and cytoprotective effects of the extracts.

Fig. 4 shows the cytoprotective effects of LsCrude and its fractions on HDF cells exposed to $CdCl_2$ at the CC_{50} (μM) level. After 24 h of pre-treatment with LsCrude (20–100 μg/mL), the relative cell viability remained above 80 % at higher extract concentrations ($\geq$ 80 μg/mL), indicating a dose-dependent cytoprotective effect (Fig. 4A). In addition, an increase in cell survival was observed when the cells were exposed to LsCrude at 100 μg/mL during both the co-treatment and post-treatment (Fig. 4B and C). This suggests that LsCrude exerts protective effects on HDF cells. Hence, 100 μg/mL of LsCrude was used for subsequent antigenotoxicity tests in all forms (pre-treatment, co-treatment, and post-treatment).

Co- or pre-treating cells with varying concentrations of LsH, LsD, LsE, and LsW (20–100 μg/mL) revealed a dose-dependent increase in cell viability that maintained cell survival above 80 % at higher extract concentrations ($\geq$ 60 μg/mL). Maximum cell viability was obtained at 80–100 μg/mL, compared to the cells treated only with $CdCl_2$ at the CC_{50} level (Fig. 4A and B). The significant increase in cell survival in the 100 μg/mL LsD co-treated group was noteworthy, compared with other treatment groups (Fig. 4B). Pre-treatment and post-treatment of LsD at varying concentrations displayed a similar but less pronounced effect relative to co-treatment, demonstrating ca. 80 % cell survival at 100 μg/mL (Fig. 4A and C, respectively). These results suggest that LsD has a wide range of protective, inhibitory, and antidotal effects against Cd-induced damage in HDF cells. The maximum cytoprotective potential was observed after co-exposure at 100 μg/mL LsD. Hence, 100 μg/mL of LsD was used for subsequent antigenotoxicity experiments in all forms (pre-treatment, co-treatment, and post-treatment).

Furthermore, co-treatment and post-treatment of HDF cells with varying concentrations of LsE (20–100 μg/mL) resulted in a significant, dose-dependent increase in cell viability. Cell survival remained above 80 % at higher extract concentrations ($\geq$ 60 μg/mL). The maximum cell survival was observed at 100 μg/mL, compared to cells treated with $CdCl_2$ at the CC_{50} level (Fig. 4B and C respectively). During pre-treatment, cell viability exhibited an inverse relationship with increasing LsE concentrations, with the highest cell survival (>80 %) observed at the lowest LsE concentration (20 μg/mL) (Fig. 4A). These findings demonstrate the broad spectrum of beneficial cytoprotective, inhibitory, and antidotal effects of LsE on HDF cells. They underscore a crucial aspect of the dual role played by natural compounds, wherein their activities can either promote or suppress, depending on the dosage employed. Therefore, antigenotoxicity assays used LsE concentrations of 20 (pre-treatment) and 100 μg/mL (co-treatment and post-treatment).

Similarly, the increased relative viability of HDF cells was positively correlated with post-treatment at increasing LsW
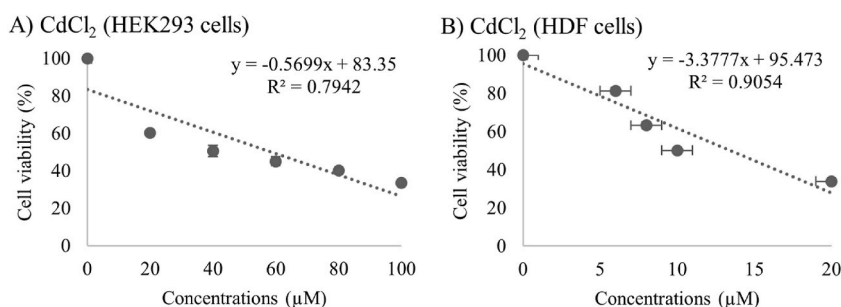

Fig. 2. Effect of cadmium at varying concentrations on cell viability of A) HEK293 renal cells and B) HDF dermal cells. Following a 24-h exposure to $CdCl_2$ at the indicated concentrations, cell viability was evaluated using the MTT assay and expressed as a percentage relative to that of the untreated cells (control). Each value represents mean $\pm$ standard deviation (n = 3) and the half maximal cytotoxicity concentration (CC_{50}) value for cadmium effect on cell survival was subsequently calculated.
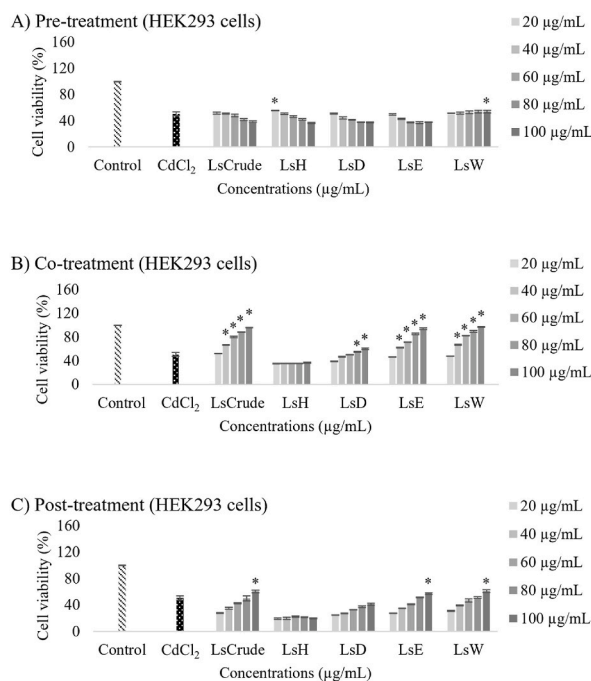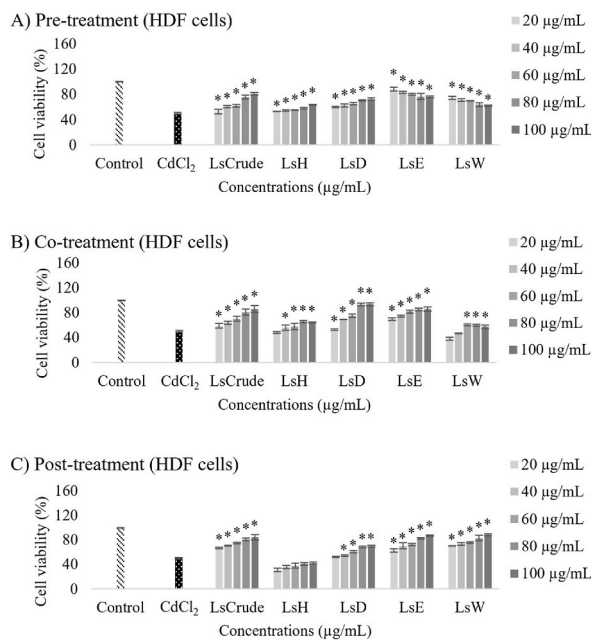
Fig. 3. Cytoprotective effects of LsCrude and its partitioned fractions (LsH, LsD, LsE and LsW) on HEK293 renal cells exposed to CdCl$_2$ at CC$_{50}$ level (40 μM) during pre-treatment, co-treatment, or post-treatment. Cell viability, indicative of cytoprotective effects, was assessed using MTT assay under three different treatment conditions: A) extract pre-incubation following Cd exposure, B) extract and CdCl$_2$ co-incubation C) extract post-incubation after Cd exposure. The relative cell viability values, expressed as mean ± standard deviation (n = 3) was compared to the untreated group (control). An asterisk (*) indicates a significant difference between the treatment group and Cd-exposed group at a *p*-value <0.05.

Fig. 4. Cytoprotective effects of LsCrude and its partitioned fractions (LsH, LsD, LsE and LsW) on HDF dermal cells exposed to CdCl$_2$ at CC$_{50}$ level (10 μM) during pre-treatment, co-treatment, or post-treatment. Cell viability, indicative of cytoprotective effects, was evaluated using MTT assay under three distinct treatment conditions: A) extract pre-incubation following Cd exposure, B) extract and CdCl$_2$ co-incubation C) extract post-incubation after Cd exposure. The relative cell viability values, expressed as mean ± standard deviation (n = 3) was compared to the untreated group (control). An asterisk (*) indicates a significant difference between the treatment group and Cd-exposed group at a *p*-value <0.05.

concentrations (20–100 μg/mL). By contrast, during pre-treatment, this viability showed an inverse relationship with the rising concentrations of LsW (Fig. 4A and C, respectively), resembling the patterns observed with LsE. Although co-treatment with LsW alone at elevated concentrations (60–100 μg/mL) alleviated Cd cytotoxicity, cell survival remained below 80 % (Fig. 4B). Thus, concentrations of 20, 80, and 100 μg/mL LsW were selected for antigenotoxicity assays (pre-treatment, co-treatment, and post-treatment, respectively).

While both pre-treatment and co-treatment with elevated LsH concentrations (20–100 μg/mL) significantly (p-value <0.05) enhanced cell survival compared to the cells treated only with $CdCl_2$ at the CC_{50} level, the increased relative viability of HDF cells at all tested concentrations still fell below 80 % for extract concentrations of 53–63 % and 48%–66 %, respectively (Fig. 4A and B). During post-treatment, LsH could not exert an antidotal effect against Cd cytotoxicity in HDF cells (Fig. 4C).

These results suggest that LsCrude and its fractions—especially co-treatment with 100LsCrude, 100LsE, or 100LsW—serve as potent suppressors of Cd-induced cytotoxicity, enhancing the viability of HEK293 cells compared to cells treated only with $CdCl_2$ at the CC_{50} level. Furthermore, LsCrude, LsD, LsE, and LsW protected, inhibited, or antidoted Cd-induced cytotoxicity in HDF cells exposed at the CC_{50} level. In particular, 20LsE in pre-treatment, 80 to 100LsD in co-treatment, and 100LsE and 100LsW in post-treatment recovered cell viability to a level comparable to the control.

3.7. Antigenotoxic effects of LsCrude and its fractions on HEK293 and HDF cells exposed to Cd, determined by the alkaline comet assay

The alkaline comet assay was used to evaluate the antigenotoxic effect of LsCrude and its fractions on HEK293 and HDF cells after Cd-exposed cells were subjected to pre-treatment, co-treatment, or post-treatment. The % DNA in the comet's tail (% tail DNA) is an indicator of primary DNA damage consistent with that caused by Cd genotoxicity and is measured using a 5-point scale scoring a total of 100 cells per sample [44,61]. CC_{50} of 40 and 10 μM $CdCl_2$ were chosen as optimal genotoxic concentrations for HEK293 and HDF cells, respectively (Fig. 2).

Figs. 5 and 7A display representative comet images along with a quantitative analysis of antigenotoxicity in HEK293 cells following co-treatment with 40 μM $CdCl_2$ and the natural compounds at the concentrations conferring maximum cytoprotective effects (100LsCrude, 100LsE, or 100LsW) (Fig. 3). Administration of the natural compounds alone resulted in no genotoxicity, as the comet-like DNA patterns of the exposed cells were comparable to those of the control (Fig. 5A). A notable increase in DNA damage was observed in the Cd-exposed cells, compared to the control. The % tail DNA for the 100LsE fraction was significantly (p-value <0.05) lower than that for the Cd-exposed group, followed by the 100LsW and 100LsCrude groups after co-treatment with Cd and the natural compounds (Fig. 5B, quantified in Fig. 7A). This suggests that the 100LsE and 100LsW fractions also mitigate DNA damage following co-exposure to Cd, consistent with the antioxidant effects attenuating the DNA-damaging ROS.

Figs. 6 and 7B depict representative comet images together with a quantitative analysis of antigenotoxicity in the HDF cells following pre-, co-, and post-treatment with 10 μM $CdCl_2$ and the natural compounds at the concentrations exhibiting the maximum
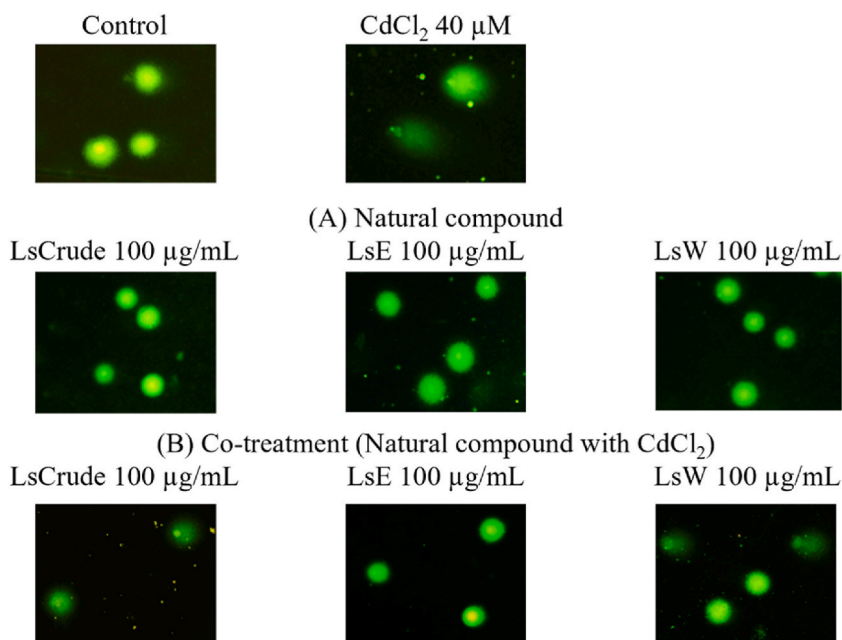

Fig. 5. Representative comet images depicting antigenotoxic effect of the LsCrude and its partitioned fractions on HEK293 cells using in vitro alkaline comet assay. The extent of DNA damage was measured in HEK293 cells treated with Cd and the tested plant extracts: A) administration of plant extracts alone at specified concentrations (100LsCrude, 100LsE, or 100LsW) for 24 h, B) co-treatment with the specified plant extracts and $CdCl_2$ at 40 μM of CC_{50} level for 24 h, in comparison to the untreated and Cd-treated group (the first panel).

cytoprotective effects (LsCrude, LsD, LsE, and LsW). Administration of the natural compounds alone resulted in no genotoxicity, as the comet-like DNA patterns of the exposed cells were comparable to that of the control (Fig. 6). On the other hand, a marked increase in DNA damage was observed in the Cd-exposed cells, compared to the control. Under pre-treatment, the % tail DNA of the 100LsD fraction was significantly lower than that in the Cd-exposed group, implying that 100LsD exhibits antigenotoxic effects against Cd toxicity (Fig. 6A). Moreover, the % tail DNA values of the 100LsD and 100LsE fractions were significantly lower than that of the Cd-exposed group, followed by the 100LsCrude and 80LsW groups after co-treatment (Fig. 6B). This result indicates that the 100LsD and 100LsE fractions are potent inhibitors of DNA damage upon co-exposure to Cd. However, this was not the case in the post-treatment groups, where the % tail DNA of groups treated with the natural compounds (100LsCrude, 100LsD, 100LsE, and 100LsW) remained comparable to that of the Cd-exposed group (Fig. 6C).

Altogether, our findings demonstrate the antigenotoxic potential of the 100LsE and 100LsW fractions in HEK293 cells during concurrent exposure to Cd. Meanwhile, the 100LsE and 100LsD fractions suppressed Cd-induced DNA damage in the HDF cells. Only the pre-treatment with the 100LsD fraction exhibited genoprotective potential against Cd toxicity in HDF cells.

3.8. Liquid chromatography-tandem mass spectrometry (LC-MS/MS) analysis

LC-MS analysis of LsCrude, LsD, LsE, and LsW revealed numerous compounds (known and novel) with potential therapeutic properties. Seventeen flavonoids and three phenolics were preliminarily identified by comparing the retention times (RT) and mass spectrometric data obtained under both negative and positive electron spray ionization modes (ESI−/ESI+), and considering mass error and data identification scores. Our results indicate that LsCrude, LsD, LsE, and LsW contain compounds similar to those found in the ethyl acetate fraction (BsE) from a previous study [30]. The identification of these constituents in the LsCrude, LsD, LsE, and LsW fractions adds to the existing data, highlighting the presence of numerous bioactive compounds (Table 3).

The LC-MS analysis confirmed the presence of phenolics and flavonoids. LsD contains gallic acid, which serves as a chemical marker for the leaves and stems of *L. strychnifolium* [29]. A 2021 study suggested that gallic acid possesses strong antioxidant properties and
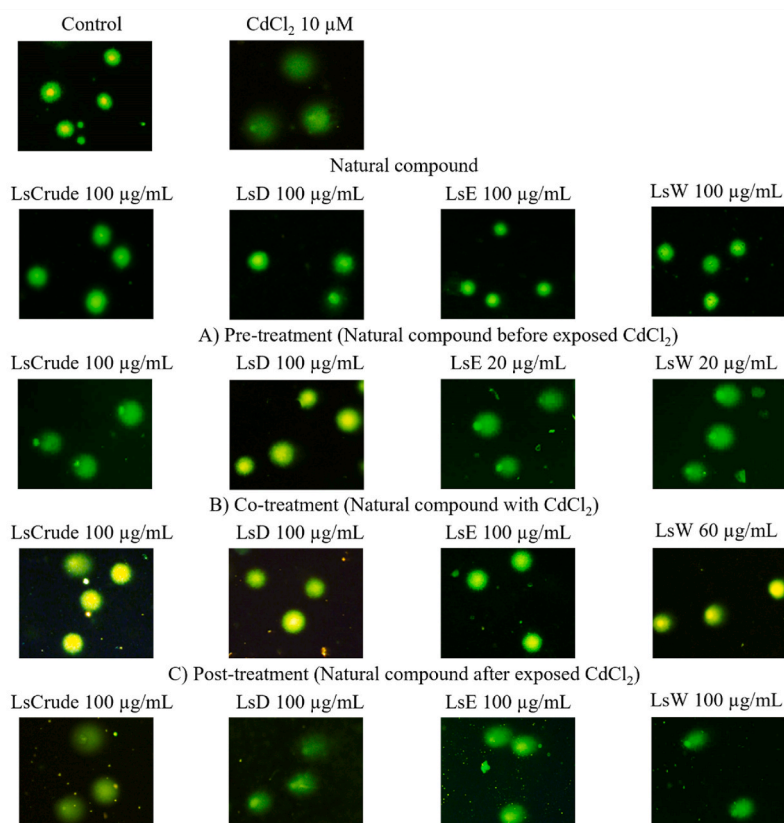
Fig. 6. Representative comet images showing antigenotoxic effect of the LsCrude and its partitioned fractions on HDF cells by in vitro alkaline comet assay. The extent of DNA damage was assessed in HDF cells treated with CdCl$_2$ at 10 μM of CC$_{50}$ level as optimal genotoxic concentration and the tested plant extracts (LsCrude, LsD, LsE, or LsW) at specified concentration: A) HDF cells were pre-treated with plant extracts (100LsCrude, 100LsD, 20LsE, and 20LsW) for 24 h, followed by CdCl$_2$ treatment for an additional 24 h, B) HDF cells were co-treated with plant extracts1 (100LsCrude, 100LsD, 100LsE, and 100LsW) along with CdCl$_2$ for 24 h, C) HDF cells were initially treated with CdCl$_2$ for 24 h, followed by plant extracts (100LsCrude, 100LsD, 100LsE, and 100LsW) for additional 24 h, in comparison to the untreated and Cd-treated group (the first-upper panel), and plant extract alone (the second-upper panel).
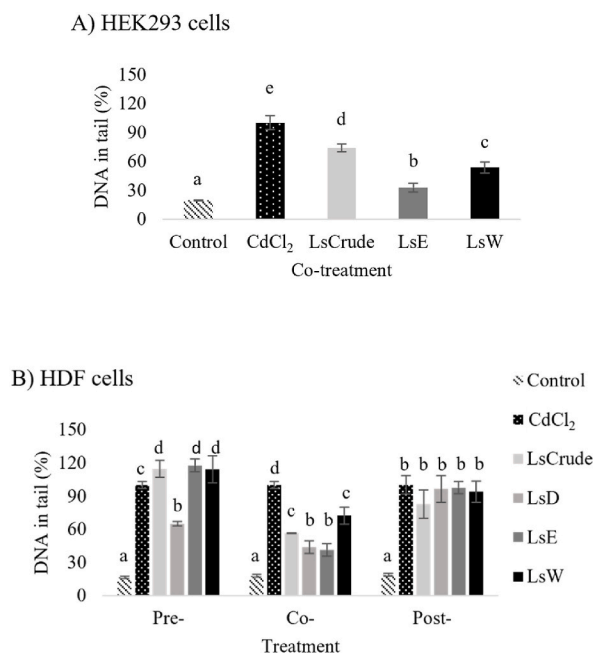
A) HEK293 cells

B) HDF cells

Fig. 7. Quantitative comet-based assessment of anti-genotoxicity of LsCrude and its selected fractions against Cd toxicity in three treatment modalities. A) HEK293 cells were co-treated with plant extracts (100LsCrude, 100LsE, and 100LsW) along with CdCl$_2$ at CC$_{50}$ level for 24 h. B) Left panel: HDF cells were pre-treated with plant extracts (100LsCrude, 100LsD, 20LsE, and 20LsW) for 24 h, followed by CdCl$_2$ treatment for an additional 24 h; Middle panel: HDF cells were co-treated with plant extracts1(100LsCrude, 100LsD, 100LsE, and 100LsW) along with CdCl$_2$ for 24 h; Right panel: HDF cells were initially treated with CdCl$_2$ for 24 h, followed by plant extracts (100LsCrude, 100LsD, 100LsE, and 100LsW) for additional 24 h. Each value is expressed as mean ± standard deviation (100 cells per comet slides). Different alphabetical letters represent significant difference between the treatment group and the Cd-exposed group at *p*-value <0.05.

may play a protective role in healthy individuals by inhibiting apoptosis [62]. Furthermore, quercetin was detected in LsD. Quercetin has antigenotoxic activity, primarily due to its ability to protect against oxidative stress and inhibit the enzymes responsible for the bioactivation of genotoxic agents, which cause oxidative DNA damage. Additional biochemical studies have suggested that quercetin's DNA-protective role is based on enhancing the antioxidant defense system by increasing the glutathione (GSH), catalase (CAT), and glutathione peroxidase (GPx) levels, and reducing oxidative stress by decreasing peroxide and NO levels [63].

Furthermore, kaempferol was identified in LsE. This flavonoid—commonly found in fruits and vegetables—is known for its anti-inflammatory, antidiabetic, antioxidant, antimicrobial, and anticancer activities [64]. The protective effect of kaempferol against CdCl$_2$-induced hepatic damage in rats is mediated by its antioxidant and anti-inflammatory effects, driven by upregulation of the Nrf2/HO-1 axis and suppression of NF-κB p65 and keap1. This mechanism suggests that the protective effects of kaempferol are mainly due to its ability to reduce oxidative stress by lowering ROS generation, increasing GSH and SOD levels via the Nrf2/HO-1 pathway, preventing mitochondrial permeability transition pore (mtPTP) opening, and suppressing NF-κB activation and inflammatory cytokine production [65].

The antioxidant potential of *L. strychnifolium* extracts and their beneficial DNA-protective effects have been previously discussed. The free radical-scavenging activity of *L. strychnifolium* extracts and their fractions was investigated. As a result, these extracts' efficacy may be attributed to their flavonoid and polyphenolic compounds, which scavenge free radicals and enhance DNA repair or synthesis [63].

In our earlier study on the anti-diabetic activity of *L. strychnifolium*, we recorded the ^{1}H and ^{13}C nuclear magnetic resonance (NMR) spectra of phytochemical compounds in the BsE. As a result, we identified phenolics and flavonoids such as gallic acid, resveratrol, catechin, taxifolin, and quercetin [30]. Here, the antioxidant effects of LsCrude and its fractions are attributed to the plant's defense systems that counteract oxidative DNA damage by donating electrons to reactive metabolites. Plant flavonoids are known as outstanding radical scavengers that mitigate DNA damage in human blood cells [66]. In addition, resveratrol, identified in BsE [30], mitigated Cd toxicity in the liver tissues of male rats by reducing Cd-induced free radicals. In a previous study, the resveratrol-treated group exhibited elevated protein levels, suggesting hepatic cellular repair [67]. The presence of flavonoids and phenolics, including resveratrol and anthocyanins, in black grape extract explains its ability to alleviate Cd-induced oxidative damage in rat livers. The intervention reversed the activities of serum hepatic markers, almost restoring them to normal levels. In addition, substantial reduction in lipid peroxidation, restoration of antioxidant levels in the liver, and enhancement of hematological parameters were reported [58]. Catechin hydrate (taxifolin), another phytochemical in LsE [30], demonstrated anti-cytogenotoxic and immunoprotective effects in Cd-treated lymphocytes. Treatment with catechin hydrate reduced the percentage of apoptotic lymphocytes while improving the viability of cells exposed to Cd (10 and 20 μM Cd) [68]. Another study reported that catechins from green tea protected rats exposed to

Table 3
Qualitative characterization of flavonoids and phenolics in LsCrude LsD, LsE and LsW fraction.

Compounds	Formula	Retention Time (min)	Mode of Ionization (ESI$^-$/ESI$^+$)	Mass	m/z	Mass Error (ppm)	Sample
Flavonoids							
1. (−)-Epigallocatechin 3-(4-methyl-gallate)	$C_{23}H_{20}O_{11}$	16.367	[M − H] $^-$	472.10	471.09	−5.97	LsCrude
2. Catechin 7-O-alpha-L-rhamnopyranoside	$C_{21}H_{24}O_{10}$	12.364	[M − H] $^-$	436.14	435.13	0.84	LsCrude
3. (−)-Epigallocatechin 3-(4-methyl-gallate)	$C_{23}H_{20}O_{11}$	16.367	[M − H] $^-$	472.10	471.09	−4.94	LsD
4. Catechin 7-O-alpha-L-rhamnopyranoside	$C_{21}H_{24}O_{10}$	17.263	[M − H] $^-$	436.14	435.13	1.43	LsD
5. Gallocatechin-(4alpha->8)-epigallocatechin	$C_{30}H_{26}O_{14}$	17.442	[M − H] $^-$	610.13	609.12	−2.96	LsD
6. Epicatechin 5-O-beta-D-glucopyranoside-3-benzoate	$C_{28}H_{28}O_{12}$	18.782	[M − H] $^-$	556.16	555.15	−0.87	LsD
7. Gallocatechin-4beta-ol	$C_{15}H_{14}O_8$	4.16	[M − H] $^-$	322.07	367.06	−8.41	LsE
8. (−)-Epigallocatechin 3-(4-methyl-gallate)	$C_{23}H_{20}O_{11}$	16.361	[M − H] $^-$	472.10	471.09	−4.87	LsE
9. Gallocatechin-(4alpha->8)-epigallocatechin	$C_{30}H_{26}O_{14}$	17.461	[M − H] $^-$	610.13	609.12	−4.32	LsE
10. Quercetin 3-(2″-galloyl-alpha-L-arabinopyranoside)	$C_{27}H_{22}O_{15}$	16.299	[M − H] $^-$	586.10	585.08	−9.33	LsD
11. Quercetin	$C_{15}H_{10}O_7$	17.89	[M − H] $^-$	302.04	301.04	−1.03	LsD
12. Quercetin 3-(2″-galloyl-alpha-L-arabinopyranoside)	$C_{27}H_{22}O_{15}$	16.311	[M − H] $^-$	586.10	585.08	−9.1	LsE
13. Kaempferol 7-O-glucoside	$C_{21}H_{20}O_{11}$	16.215	[M − H] $^-$	448.10	447.09	0.15	LsE
14. Kaempferol 3-(2″-galloyl-alpha-L-arabinopyranoside)	$C_{27}H_{22}O_{14}$	16.898	[M − H] $^-$	570.10	569.09	−8.32	LsE
15. Kaempferol 3-(3″-p-coumaroylrhamnoside)-7-rhamnoside	$C_{36}H_{36}O_{16}$	17.163	[M − H] $^-$	724.20	723.19	−0.47	LsE
16. Kaempferol	$C_{15}H_{10}O_6$	18.473	[M − H] $^-$	286.05	285.04	−1.05	LsE
17. Luteolin	$C_{15}H_{10}O_6$	17.812	[M − H] $^-$	286.05	285.04	1.43	LsD
18. Luteolin	$C_{15}H_{10}O_6$	17.84	[M − H] $^-$	286.05	285.04	1.15	LsE
19. 2′,3,5,6′,7-Pentahydroxyflavanone	$C_{15}H_{12}O_7$	16.152	[M − H] $^-$	304.06	303.05	−0.79	LsCrude
20. 2,6,7,4′-Tetrahydroxyisoflavanone	$C_{15}H_{12}O_6$	17.255	[M − H] $^-$	288.06	287.06	−0.72	LsCrude
21. 2,5-Dihydroxy-7-methoxy-8-methylflavanone	$C_{17}H_{16}O_5$	19.342	[M − H] $^-$	300.10	299.09	1.81	LsCrude
22. 2′,3,5,6′,7-Pentahydroxyflavanone	$C_{15}H_{12}O_7$	16.175	[M − H] $^-$	304.06	303.05	−0.38	LsD
23. 2,5-Dihydroxy-7-methoxy-8-methylflavanone	$C_{17}H_{16}O_5$	19.337	[M − H] $^-$	300.10	299.09	1.02	LsD
24. 2′,3,5,6′,7-Pentahydroxyflavanone	$C_{15}H_{12}O_7$	16.207	[M − H] $^-$	304.06	303.05	−0.99	LsE
25. Euchrestaflavanone A	$C_{25}H_{28}O_5$	21.226	[M − H] $^-$	408.19	407.19	0.39	LsE
26. Uvarinol	$C_{36}H_{30}O_7$	15.753	[M − H] $^-$	574.20	575.21	−1.73	LsW
Phenolics							
27. Gallic acid	$C_7H_6O_5$	13.533	[M − H] $^-$	170.02	169.01	−0.62	LsD
28. Resveratrol 4'-(2-galloylglucoside)	$C_{27}H_{26}O_{12}$	16.532	[M − H] $^-$	542.14	541.14	0.55	LsD
29. Resveratrol 4'-(2-galloylglucoside)	$C_{27}H_{26}O_{12}$	16.482	[M − H] $^-$	542.14	541.14	0.3	LsE
30. Kelampayoside A	$C_{20}H_{30}O_{13}$	9.572	[M + HCOO] $^-$	478.17	501.15	−7.96	LsW

Cd against bone metabolic abnormalities [69]. Quercetin, present in LsE [30], reduced Cd-mediated DNA damage in goat testicular cells, as evidenced by a decreased % tail DNA in the comet assay in the quercetin-supplemented groups after 8 h of exposure to Cd (50 and 100 μM) [70]. Another study demonstrated the protective effect of bioflavonoids such as quercetin in mitigating Cd-induced oxidative stress-related renal dysfunction in rats, attributed to a diminishing rate of lipid peroxidation. Thus, the treatment alleviated the Cd-mediated biochemical alterations and pathological changes observed in rat serum, urine, and tissues [71].

Overall, the published data agree with our findings, suggesting that the polyphenolic compounds from *L. strychnifolium* likely contribute to protecting human renal and dermal cells from toxic metal-induced ROS.

4. Conclusions

This is the first report on the anti-cytogenotoxic activities of *L. strychnifolium* extract against Cd exposure at the CC$_{50}$ (μM) level in vitro. An alkaline comet assay was performed using HEK293 renal and HDF dermal cell models. Our results demonstrate the effectiveness of the dichloromethane and ethyl acetate fractions in preventing Cd-induced damage to HEK293 cells during co-treatment.

The LsD fraction demonstrated cyto-geno-protective effects against Cd toxicity at the CC_{50} (µM) level in the pre-treatment of HDF cells. The HDF cells co-treated with the LsCrude or the LsD or LsE fractions suppressed Cd-induced DNA damage. These anti-cytogenotoxic effects are likely due to the antioxidant activities of the phytochemicals in the extracts, as evidenced by DPPH and FRAP assays, phytochemical screening, and LC-MS analysis. Gallic acid, quercetin, and kaempferol may be the active compounds responsible for these anti-cytogenotoxic effects. These results demonstrate the effectiveness of *L. strychnifolium* extracts in mitigating Cd toxicity and support the use of *L. strychnifolium* in Thai traditional medicine. Our findings encourage the further exploration and identification of bioactive compounds and responsive gene expression to develop health supplements and targeted therapeutic agents.

Data availability statement

The original data in this article will be made available on request or directed to the corresponding author.

CRediT authorship contribution statement

Pattaravan Maliyam: Writing – review & editing, Writing – original draft, Visualization, Investigation, Formal analysis, Data curation. **Surat Laphookhieo:** Writing – review & editing, Validation, Supervision, Data curation. **Preeyaporn Koedrith:** Writing – review & editing, Validation, Supervision, Data curation. **Panupong Puttarak:** Writing – review & editing, Writing – original draft, Supervision, Software, Resources, Project administration, Methodology, Investigation, Funding acquisition, Data curation, Conceptualization.

Declaration of competing interest

Acknowledgements

References

[1] Y. Song, W. Li, Y. Xue, H. Zhou, W. Wang, C. Liu, Impact of industrial pollution of cadmium on traditional crop planting areas and land management: a case study in northwest China, Land 10 (12) (2021) 1364.

[2] H. Zhang, M. Reynolds, Cadmium exposure in living organisms: a short review, Sci. Total Environ. 678 (2019) 761–767, https://doi.org/10.1016/j.scitotenv.2019.04.395.

[3] E.R. Chellaiah, Cadmium (heavy metals) bioremediation by Pseudomonas aeruginosa: a minireview, Appl. Water Sci. 8 (6) (2018). https://link.gale.com/apps/doc/A553948122/AONE?u=anon8e79626&sid=googleScholar&xid=d7e3fa57.

[4] F.U. Haider, C. Liqun, J.A. Coulter, S.A. Cheema, J. Wu, R. Zhang, M. Wenjun, M. Farooq, Cadmium toxicity in plants: impacts and remediation strategies, Ecotoxicol. Environ. Saf. 211 (2021) 111887, https://doi.org/10.1016/j.ecoenv.2020.111887.

[5] S. Satarug, Dietary Cadmium intake and its effects on kidneys, Toxics 10 (6) (2018) 15.

[6] S. Satarug, S.H. Garrett, M.A. Sens, D.A. Sens, Cadmium, environmental exposure and health outcomes, Environ. Health Perspect. 118 (2010) 182–190.

[7] European Food Safety Authority (EFSA), Scientific opinion of the panel on contaminants in the food chain on a request from the European Commission on cadmium in food, EFSA 980 (2009) 1–139.

[8] G. Genchi, M.S. Sinicropi, G. Lauria, A. Carocci, A. Catalano, The effects of cadmium toxicity, Int. J. Environ. Res. Publ. Health 17 (11) (2020) 3782.

[9] Y.O. Son, J.C. Lee, J.A. Hitron, J. Pan, Z. Zhang, X. Shi, Cadmium induces intracellular $Ca2+$- and H_2O_2-dependent apoptosis through JNK- and p53-mediated pathways in skin epidermal cell line, Toxicol. Sci. 113 (1) (2010) 127–137.

[10] Iarc. IARC monographs on the evaluation of carcinogenic risks to humans-beryllium, cadmium, mercury, and exposures in the glass manufacturing industry, in: Summary of Data Reported and Evaluation, vol. 58, International Agency for Cancer Research-World Health Organization, Geneva, Switzerland, 1997.

[11] R. Thirugnanasampandan, R. Jayakumar, Protection of cadmium chloride induced DNA damage by Lamiaceae plants, Asian Pac. J. Trop. Biomed. 1 (5) (2011) 391–394, https://doi.org/10.1016/S2221-1691(11)60086-5.

[12] P. Joseph, Mechanisms of cadmium carcinogenesis, Toxicol. Appl. Pharmacol. 238 (3) (2009) 272–279, https://doi.org/10.1016/j.taap.2009.01.011.

[13] Hong Yang, Shu Yan, Cadmium transporters in the kidney and cadmium-induced nephrotoxicity, Int. J. Mol. Sci. 16 (1) (2015) 1484–1494, https://doi.org/10.3390/ijms16011484.

[14] P. Mahajan, J. Kaushal, Role of phytoremediation in reducing cadmium toxicity in soil and water, J. Toxicol. 2018 (2018) 4864365, https://doi.org/10.1155/2018/4864365.

[15] A. Akesson, T. Lundh, M. Vahter, P. Bjellerup, J. Lidfeldt, C. Nerbrand, G. Samsioe, U. Strömberg, S. Skerfving, Tubular and glomerular kidney effects in Swedish women with low environmental cadmium exposure, Environ. Health Perspect. 113 (11) (2005) 1627–1631, https://doi.org/10.1289/ehp.8033.

[16] E.Y. Hernández-Cruz, I. Amador-Martínez, A.K. Aranda-Rivera, A. Cruz-Gregorio, J. Pedraza Chaverri, Renal damage induced by cadmium and its possible therapy by mitochondrial transplantation, Chem. Biol. Interact. 361 (2022) 109961, https://doi.org/10.1016/j.cbi.2022.109961.

[17] A.A. Tinkov, T. Filippini, O.P. Ajsuvakovae, M.G. Skalnaya, J. Aasethf, G. Bjørklundh, E.R. Gatiatulinai, E.V. Popova, O.N. Nemereshinai, P.T. Huangk, et al., Cadmium and atherosclerosis: a review of toxicological mechanisms and a meta-analysis of epidemiologic studies, Environ. Res. 162 (2018) 240–260.

[18] M. Kauth, O.V. Trusova, Topical ectoine application in children and adults to treat inflammatory diseases associated with an impaired skin barrier: a systematic review, Dermatology and therapy 12 (2) (2022) 295–313, https://doi.org/10.1007/s13555-021-00676-9.

[19] R. Bahri, D. Saidane-Mosbahi, M. Rouabhia, Cytokine release and cytotoxicity in human keratinocytes Induced by polycyclic aromatic hydrocarbons (1-Methylpyrene and Perylene), J. Toxicol. Environ. Health, Part A 73 (2010) 552–564.

[20] L. Chavatte, M. Juan, S. Mounicou, E. Leblanc Noblesse, K. Pays, C. Nizard, A.L. Bulteau, Elemental and molecular imaging of human full thickness skin after exposure to heavy metals, Metallomics : integrated biometal science 12 (10) (2020) 1555–1562, https://doi.org/10.1039/d0mt00121j.

[21] W. Du, Y. Dong, Z. Wang, et al., Study on the mechanism of cadmium chloride pollution accelerating skin tissue metabolism disorder, aging and inhibiting hair regeneration, Front. Public Health 10 (2022) 1035301, https://doi.org/10.3389/fpubh.2022.1035301. Published 2022 Oct 19.

[22] S.J. Yoon, C.J. Lim, H.-J. Chung, J.-H. Kim, Y.H. Huh, K. Park, S. Jeong, Autophagy activation by *crepidiastrum denticulatum* extract attenuates environmental pollutant-induced damage in dermal fibroblasts, Int. J. Mol. Sci. 20 (3) (2019) 517.

[23] A. Boon-young, P. Bootdawan, K. Bunluepuech, S. Tewtrakul, S. Kraithep, Antioxidant activity of *Bauhinia strychnifolia* extract. The 3rdNEU National and International Conference 2015 "Integrated Enhances Sustainable Knowledge, 2015, pp. 546–552.

[24] W. Lertpongpipat, D. Chaiyakhun, Comparison of effectiveness on increasing cholinesterase blood level between *Thunbergiaceae* and *Bauhinia strychnifolia* craib in agriculturists, Journal of the Office of DPC 7 Khon Kaen 18 (3) (2011) 49–58.

[25] S. Sayompark, A. Itharat, P. Hansakul. Comparative study of antioxidant activities and total phenolic content of *Bauhinia strychnifolia* leaves extracts, Proceeding of 1ˢᵗ Conference on Graduate Student Network of Thailand, Sci-Health, Bangkok, Thailand, 2012 011.

[26] A. Itharat, S. Sayompark, P. Hansakul, B. Dechayont, In vitro antioxidant activities of extracts of *Bauhinia strychnifolia* stems and leaves: comparison with activities in green tea extracts, Med. Aromatic Plants 5 (2016) 243.

[27] S. Yuenyongsawad, K. Bunluepuech, C. Wattanapiromsakul, S. Tewtrakul, Anti-cancer activity of compounds from *Bauhinia strychnifolia* stem, Ethnopharmacology 150 (2013) 765–769.

[28] C. Panchinda, S. Ruangnoo, A. Itharat, Cytotoxic activity against cancer cell lines from the ethanolic extracts and its VLC fractions of Bauhinia strychnifolia leaves, J. Med. Assoc. Thail. 99 (Suppl 4) (2016) S110–S115.

[29] S. Kongkiatpaiboon, HPLC quantification of chemical markers from Lysiphyllum strychnifolium, Retrieved from, https://repository.li.mahidol.ac.th/handle/123456789/86871, 2022.

[30] R. Praparatana, P. Maliyam, L.R. Barrows, P. Puttarak, Flavonoids and phenols, the potential anti-diabetic compounds from *Bauhinia strychnifolia* craib, Stem. Molecules 27 (2022) 2393.

[31] A.A. Alshatwi, T.N. Hasan, A.M. Alqahtani, N.A. Syed, G. Shafi, A.H. Al-Assaf, A.S. Al-Khalifa, Delineating the anti-cytotoxic and anti-genotoxic potentials of catechin hydrate against cadmium toxicity in human peripheral blood lymphocytes, Environ. Toxicol. Pharmacol. 38 (2) (2014) 653–662, https://doi.org/10.1016/j.etap.2014.07.013.

[32] H. Panchal, J.K. Bhardwaj, Quercetin supplementation alleviates cadmium induced genotoxicity-mediated apoptosis in caprine testicular cells, Biol. Trace Elem. Res. (2023), https://doi.org/10.1007/s12011-023-04038-8.

[33] Al-Baqami NM, Hamza RZ. Protective effect of resveratrol against hepatotoxicity of cadmium in male rats: antioxidant and histopathological approaches. 2021. Coatings. 11(5), 594.

[34] Kingkan Bunluepuech, Wattanapiromsakul Chatchai, Fameera Madaka, Supinya Tewtrakul, Anti-HIV-1 integrase and anti-allergic activities of Bauhinia strychnifolia, Songklanakarin J. Sci. Technol. 35 (2013) 659–664.

[35] W. Pichayakorn, C. Monton, Y. Sampaopan, K. Panrat, J. Suksaeree, Fabrication and characterization of buccal film loaded self-emulsifying drug delivery system containing *Lysiphyllum strychnifolium* stem extracts, AAPS PharmSciTech 23 (6) (2022) 194, https://doi.org/10.1208/s12249-022-02341-6.

[36] A.K. Pandey, S. Tripathi, Concept of standardization, extraction and pre phytochemical screening strategies for herbal drug, J. Pharmacogn. Phytochem. 2 (2014) 115–119.

[37] N. Jiangseubchatveera, S. Liawruangrath, A. Teerawutgulrag, D. Santiarworn, S.G. Pyne, B. Liawruangrath, Phytochemical screening, phenolic and flavonoid contents, antioxidant and cytotoxic activities of *Graptophyllum pictum* (L.) Griff, Chiang Mai J. Sci. 44 (2017) 193–202.

[38] N.L. BaoDuy, N.K. Pham, M. Trang, Preliminary phytochemical analysis of leaf extracts ofthuja orientalis (L.) endl, Int. j. res. sci. manag (2015) 21–25.

[39] M.M. Sakyiamah, P.K. Gordon, P. Bolah, et al., Assessment of the phytochemical composition and antimicrobial properties of Tapinanthus bangwensis leaves hosted by the branches of Persea americana, BMC Complement Med Ther 23 (1) (2023) 34, https://doi.org/10.1186/s12906-023-03860-w. Published 2023 Feb 3.

[40] B.A. Purba, R. Pujiarti, M. Masendra, G. Lukmandaru, Total phenolic, flavonoid, tannin content and DPPH scavenging activity of *Caesalpinia sappan* linn, Bark, Wood Res. J. 13 (2) (2023) 63–68.

[41] T. Maulana, Syamsul Falah, Dimas Andrianto, Total phenolic content, total flavonoid content, and antioxidant activity of water and ethanol extract from Surian (Toona sinensis) leaves, IOP Conf. Ser. Earth Environ. Sci. 299 (2019) 012021, https://doi.org/10.1088/1755-1315/299/1/012021.

[42] M. Kaji, P. Puttarak, Development of standardized *Cyanthillium cinereum* (L.) H. Rob. Extract and determination of its biological activities, J. Nat. Prod. 12 (2022) 46–54.

[43] N.B. Gaber, S.I. El-Dahy, E.A. Shalaby, Comparison of ABTS, DPPH, permanganate, and methylene blue assays for determining antioxidant potential of successive extracts from pomegranate and guava residues, Biomass Conv. Bioref. 13 (2023) 4011–4020, https://doi.org/10.1007/s13399-021-01386-0.

[44] R. Chomchan, S. Siripongvutikorn, P. Maliyam, B. Saibandith, P. Puttarak, Protective effect of selenium-enriched ricegrass juice against cadmium-induced toxicity and DNA damage in HEK293 kidney cells, Foods 7 (2018) 81.

[45] X. Duan, T. Wu, T. Liu, H. Yang, X. Ding, Y. Chen, Y. Mu, Vicenin-2 ameliorates oxidative damage and photoaging via modulation of MAPKs and MMPs signaling in UVB radiation exposed human skin cells, J. Photochem. Photobiol. B Biol. 190 (2019) 76–85, https://doi.org/10.1016/j.jphotobiol.2018.11.018.

[46] M.M. Hoshina, M.A. Marin-Morales, Anti-genotoxicity and anti-mutagenicity of Apis mellifera venom. Mutation research, Genetic toxicology and environmental mutagenesis 762 (2014) 43–48, https://doi.org/10.1016/j.mrgentox.2014.11.005.

[47] T. Cavaş, S. Könen, Detection of cytogenetic and DNA damage in peripheral erythrocytes of goldfish (Carassius auratus) exposed to a glyphosate formulation using the micronucleus test and the comet assay, Mutagenesis 22 (4) (2007) 263–268, https://doi.org/10.1093/mutage/gem012.

[48] Natalia Bailon-Moscoso, Juan Carlos Romero Benavides, María Isabel Ramirez Orellana, Karla Ojeda, Glenda Granda, Edward A. Ratovski, Patricia Ostrosky-Wegman, Cytotoxic and genotoxic effects of extracts from Annona Montana M. fruit, Food Agric. Immunol. 27 (4) (2016) 559–569, https://doi.org/10.1080/09540105.2016.1148121.

[49] P. Widyawati, Tarsisius Budianta, F.A. Kusuma, E.L. Wijaya, Difference of solvent polarity to phytochemical content and antioxidant activity of *Pluchea indica less* leaves extracts, Int. J. Pharmacogn. Phytochem. Res. 6 (2014) 850–855.

[50] Kingkan Bunluepuech, Wattanapiromsakul Chatchai, Fameera Madaka, Supinya Tewtrakul, Anti-HIV-1 integrase and anti-allergic activities of Bauhinia strychnifolia, Songklanakarin J. Sci. Technol. 35 (2013) 659–664.

[51] M.G. Mostofa, A.S.M.A. Reza, Z. Khan, M.S. Munira, M.M. Khatoon, S.R. Kabir, M.G. Sadik, D. Ağagündüz, R. Capasso, M. Kazi, A.K. Alam, Apoptosis-inducing anti-proliferative and quantitative phytochemical profiling with in silico study of antioxidant-rich Leea aequata L. leaves, Heliyon 10 (1) (2023) e23400, https://doi.org/10.1016/j.heliyon.2023.e23400.

[52] S.J. Padayatty, A. Katz, Y. Wang, P. Eck, O. Kwon, J.H. Lee, S. Chen, C. Corpe, A. Dutta, S.K. Dutta, M. Levine, Vitamin C as an antioxidant: evaluation of its role in disease prevention, J. Am. Coll. Nutr. 22 (1) (2003) 18–35, https://doi.org/10.1080/07315724.2003.10719272.

[53] S. Phongpaichit, J. Nikom, N. Rungjindamai, J. Sakayaroj, N. Hutadilok-Towatana, V. Rukachaisirikul, K. Kirtikara, Biological activities of extracts from endophytic fungi isolated from Garcinia plants, FEMS Immunol. Med. Microbiol. 51 (3) (2007) 517–525.

[54] C. Kairupan, Feky Mantiri, R. Rumende, Phytochemical screening and antioxidant activity of ethanol extract of leilem (clerodendrum minahassae teijsm. & binn) as an antihyperlipidemic and antiatherosclerotic agent, Earth Environ. Sci. 217 (2019) 012016.

[55] S.H. Qari, Evaluation of the antioxidant activity, genotoxic, and cytotoxic effects of the ethanolic leaves extract of Abutilon hirtum (Lam.) Sweet using in vitro assays, Heliyon 9 (8) (2023) e18617.

[56] Afroze Meena, Shanta Ahmed, Taksim Uddin, Nasir Majumder, Senjuti Hossain, Md Rana, Phytochemical screening and in vitro determination of antioxidant potential of methanolic extract of Streospermum chelonoides, J. Appl. Pharmaceut. Sci. 3 (2013) 117–121.

[57] J. Ezzati Nazhad Dolatabadi, A. Mokhtarzadeh, S.M. Ghareghoran, G. Dehghan, Synthesis, characterization and antioxidant property of quercetin-Tb (III) complex, Adv. Pharmaceut. Bull. 4 (2) (2014) 101–104, https://doi.org/10.5681/apb.2014.016.

[58] Ilham ELOTHMANI. Hmid, Driss Hanine, Hafida Oukabli, Ahmed, Emira Mehinagic, Comparative study of phenolic compounds and their antioxidant attributes of eighteen pomegranate (*Punica granatum* L.) cultivars grown in Morocco, Arab. J. Chem. 113 (10) (2013) 1016.

[59] M.H. Labiad, Harhar Hicham, A. Ghanimi, Mohamed Tabyaoui, Phytochemical screening and antioxidant activity of Moroccan *Thymus satureioïdes* extracts, J. Mater. Environ. Sci. 8 (2017) 2132–2139.

[60] J. López-García, M. Lehocký, P. Humpolíček, P. Sáha, HaCaT keratinocytes response on antimicrobial atelocollagen substrates: extent of cytotoxicity, cell viability and proliferation, J. Funct. Biomater. 5 (2014) 43–57.

[61] A.M. Sandbichler, M. Höckner, Cadmium protection strategies—a hidden trade-off? Int. J. Mol. Sci. 17 (1) (2016) 1–22.

[62] A.C. G, R. Gondru, Y. Li, J. Banothu, Coumarin-benzimidazole hybrids: a review of developments in medicinal chemistry, Eur. J. Med. Chem. 227 (2022) 113921, https://doi.org/10.1016/j.ejmech.2021.113921.

[63] I.A. Kassem, A.A. Farghaly, N.S. Ghaly, Z.M. Hassan, M. Nabil, Composition and genoprotective effect of the flavonoidal content of Lepidium sativum L. methanolic seed extract against cyclophosphamide-induced DNA damage in mice, Phcog. J. 12 (1) (2020).

[64] N. Sharma, S. Biswas, N. Al-Dayan, A.S. Alhegaili, M. Sarwat, Antioxidant role of kaempferol in prevention of hepatocellular carcinoma, Antioxidants 10 (9) (2021) 1419, https://doi.org/10.3390/antiox10091419.

[65] A.S. Alshehri, A.F. El-Kott, M.S.A. El-Gerbed, A.E. El-Kenawy, G.M. Albadrani, H.S. Khalifa, Kaempferol prevents cadmium chloride-induced liver damage by upregulating Nrf2 and suppressing NF-κB and keap1, Environ. Sci. Pollut. Res. Int. 29 (10) (2022) 13917–13929, https://doi.org/10.1007/s11356-021-16711-3.

[66] N. Devipriya, A.R. Sudheer, M. Srinivasan, V.P. Menon, Quercetin ameliorates gamma radiation-induced DNA damage and biochemical changes in human peripheral blood lymphocytes, Mutat. Res. Genet. Toxicol. Environ. Mutagen 654 (1) (2008) 1–7.

[67] Al-Baqami NM, Hamza RZ. Protective effect of resveratrol against hepatotoxicity of cadmium in male rats: antioxidant and histopathological approaches. 2021. Coatings. 11(5), 594.

[68] A.A. Alshatwi, T.N. Hasan, A.M. Alqahtani, N.A. Syed, G. Shafi, A.H. Al-Assaf, A.S. Al-Khalifa, Delineating the anti-cytotoxic and anti-genotoxic potentials of catechin hydrate against cadmium toxicity in human peripheral blood lymphocytes, Environ. Toxicol. Pharmacol. 38 (2) (2014) 653–662.

[69] J.H. Choi, I.K. Rhee, K.Y. Park, K.Y. Park, J.K. Kim, S.J. Rhee, Action of green tea catechin on bone metabolic disorder in chronic cadmium-poisoned rats, Life Sci. 73 (12) (2003) 1479–1489.

[70] H. Panchal, J.K. Bhardwaj, Quercetin supplementation alleviates cadmium induced genotoxicity-mediated apoptosis in caprine testicular cells, Biol. Trace Elem. Res. (2023), https://doi.org/10.1007/s12011-023-04038-8.

[71] J. Renugadevi, S.M. Prabu, Quercetin protects against oxidative stress-related renal dysfunction by cadmium in rats, Exp. Toxicol. Pathol. 62 (5) (2010) 471–481.